Journal of Applied Polymer Science

Nanocomposites of PVC/TiO_2 Nanorods: Surface Tension and Mechanical Properties Before and After UV Exposure

Parvane Sokhandani,[1,2] Ali Akbar Babaluo,[1] Mostafa Rezaei,[2] Mehdi Shahrezaei,[1] Amin Hasanzadeh,[1,2] Shadi Ghaebi Mehmandoust,[1] Reza Mehdizadeh[1,2]

[1]Nanostructure Material Research Center, Chemical Engineering Department, Sahand University of Technology, Tabriz, Iran
[2]Institute of Polymeric Materials, Polymer Engineering Department, Sahand University of Technology, Tabriz, Iran
Correspondence to: A. A. Babaluo (E-mail: a.babaluo@sut.ac.ir)

ABSTRACT: In this study, nanocomposites of poly(vinyl chloride) (PVC), using the synthesized titanium dioxide (TiO_2) nanorods and commercial nanopowder of titanium dioxide (Degussa P25) were produced by melt blending. The presence of TiO_2 nanorods in PVC matrix led to an improvement in mechanical properties of PVC nanocomposites in comparison with unfilled PVC. The photocatalytic degradation behavior of PVC nanocomposites were investigated by measuring their structural change evaluations, surface tension, and mechanical properties before and after UV exposure for 500 h. It was found that mechanical and physical properties of PVC nanocomposites are not reduced significantly after UV exposure in the presence of TiO_2 nanorods in comparison with the presence of TiO_2 nanoparticles, which can be due to the amorphous structure of the synthesized nanorods. Therefore, it can be concluded that TiO_2 nanorods led to an improvement in photostability and mechanical properties of PVC nanocomposites. The interfacial adhesion between TiO_2 nanorods and PVC matrix was also investigated. © 2013 Wiley Periodicals, Inc. J. Appl. Polym. Sci. 129: 3265–3272, 2013

KEYWORDS: poly(vinyl chloride); mechanical properties; degradation

Received 6 July 2012; accepted 1 January 2013; published online 21 February 2013
DOI: 10.1002/app.38989

INTRODUCTION

Poly(vinyl chloride) (PVC) is one of the most important and widely in use thermoplastics because of its valuable properties, such as low production cost, good process ability, easy modification and excellent chemical and fire resistance.[1,2] The ultimate user acceptance of poly (vinyl chloride) products for outdoor building applications will depend on their stability to resist deterioration of their mechanical and aesthetic properties over long periods of exposure that is needed to a careful compounding.[3] As a kind of typical brittle materials, PVC has been modified to extend its applications, and many impact modifiers have been commercialized and used for many years, such as chlorinated polyetyhylene (CPE), acrylonytrile butadiene styrene (ABS), poly (methyl-methacrylate-co-methacrylate) (ACR).[4–7] Inorganic particles have also been used to modify the mechanical properties of PVC. It is well known that the shape, size, filler content and the adhesion of particle/matrix interfaces strongly affect the mechanical properties and the fracture behavior of composites.[8,9]

On the other hand, production of materials in nanometric dimensions shows unique properties compared to bulk materials that provide high potential of research in this field. For example, it has been found that the addition of calcium carbonate nanopowder significantly improves both the toughness and stiffness of PVC, while having slight effect on the tensile strength reduction.[10] Also, the addition of the silica nanoparticles improved the mechanical properties in some composites.[11]One of the most interesting researches in this field, is producing TiO_2 in nanometric dimensions which can be due to its desirable chemical and physical properties resulting in its wide applications in different fields such as photocatalysts, catalytic supports, polymeric nanocomposites, gas sensors, etc.[12–14] One dimensional nanostructure materials such as nanotubes and nanorods have attractive properties because of their special geometric shape that causes continuously extends their applications. So, desirable properties of TiO_2 as well as intrinsic properties of nanorods provide wide researches on this type of nanostructures.[15–17]

The improvement of mechanical properties of PVC reinforced with nanorods is believed relates to the high aspect ratio (*l/d*) of these materials. Then, the addition of TiO_2 nanorods to PVC matrix could improve its mechanical properties, but photocatalytic property of TiO_2 would negatively affect on mechanical properties of PVC.[18,19] Therefore, high aspect ratio (*l/d*) with relatively low photocatalytic property, make TiO_2 nanorods ideal candidate as reinforcement materials in PVC composites.

Table I. Composition of the Prepared PVC Nanocomposites

Name	PVC (phr)	Sample of TiO_2				$CaCO_3$ (phr)	$CaSt_2$ (phr)	$ZnSt_2$ (phr)	Parafine wax (phr)	StAc (phr)
		Sample	TiO_2 (phr)	Aspect ratio *l*/*d*	Specific surface area (m^2/g)					
NP1	100	PTi1 (nanorod)	3	>11.8	20	5	2.5	2.5	2.8	0.22
NP2	100	PTi2 (nanorod)	3	9.5	35	5	2.5	2.5	2.8	0.22
NP3	100	P25 (nanoparticle)	3		52.4	5	2.5	2.5	2.8	0.22

However, the effective utilization of them in composites depends on their ability to disperse homogenously throughout the matrix without destroying their integrity. Furthermore, good interfacial bonding is required to achieve the proper mechanical properties of the composite.[20] Therefore, study on the nanocomposites of PVC/TiO_2 nanorods still remains a matter of interest, but a few studies have been done on this field in the literature.

In this study, we looked for ascertaining the changes in the mechanical properties of PVC with the addition of TiO_2 nanorods, as well as the photocatalytic degradation of PVC nanocomposites were investigated with the presence of the synthesized TiO_2 nanorods and commercial TiO_2 nanoparticles (Degussa, P25) compared to unfilled PVC. Nanocomposites of PVC were prepared by melt compounding. The effects of photodegradation of PVC nanocomposites were evaluated by measuring tensile strength data (experimentally and theoretically), structural changes, and surface tension of nanocomposites before and after UV exposure. The interfacial adhesion between TiO_2 nanorods and PVC matrix was determined by the interfacial interaction parameter (β).

EXPERIMENTAL

Materials

Poly(vinylchloride) (PVC) (Bandar Imam Petro., Iran) (K value 64-66) as polymer matrix, titanium dioxide (TiO_2) with two different structures (P25 nanoparticles from Degussa, Germany. and homemade nanorods) as modifier, calcium carbonate ($CaCO_3$) (Poodrkar, Iran) as filler, calcium stearate ($CaSt_2$) and zinc stearate ($ZnSt_2$) (Poodrkar, Iran) as thermal stabilizer, paraffin wax (Poodrkar, Iran) as internal lubricant and stearic acid (StAc) (EPS IMPEX, Malaysia) as external lubricant were used to prepare PVC nanocomposite compounds.

Preparation of TiO_2 Nanorodes

Titanium dioxide nanorods were synthesized from the Commercial titanium dioxide (P25 nanoparticles from Degussa, Germany) nanopowder. The Commercial titanium dioxide nanopowder was added to sodium hydroxide (NaOH, %99 Merck, Germany) solution and then was poured into the Teflon holder of autoclave. The reaction time in the autoclave was 24 h and the temperature of it was 150°C. The filtered material was thoroughly washed with distilled water until the washing solution achieved pH 7. Then, sample was washed with sulfuric acid (H_2SO_4, %98 Merck, Germany) and distilled water, respectively. The sample was dried in vacuum oven in the temperature of 80°C. The difference between synthesized TiO_2 nanorods is related to the initial concentration of Commercial TiO_2 nanopowder that was 0.8 g for PTi1 and 0.4 g for PTi2.

Preparation of PVC/ TiO_2 Nanocomposites

PVC nanocomposites were prepared according to Table I. Dry powder blends were premixed and heated from room temperature to 120°C over ~12 min. Dry blends were processed using an internal mixer (Brabender, W50EHT, Plasti-corder, Germany) (with a rotor speed of 60 rpm), and temperature of 170°C, for 8 min. The resulting compound was then molded into rectangular sheets by compression molding at 170°C and 5 MPa pressure for 5 min using a hot press (Brabender, Polystat 200 T, Germany).

Artificial Weathering

The artificially simulated weathering was carried out using a (TL 20 W/05, Philips, Germany) ultraviolet (UV) exposure lamp. The samples were artificially aged in UV chambers, for 500 h with continuous UV irradiation. The relative humidity was 60–70% and the temperature was 25°C in the chambers. The irradiation distance between the lamp and the samples was 25 cm. The intensity of incident radiation was 320 W/m^2.

Characterization

Characterization of TiO_2 Nanorods and Nanoparticles. Nitrogen adsorption analysis (BET) was performed with CHEMBET-3000 apparatus. The surface morphology of nanorods was examined using VEGA\\TESCAN scanning electron microscopy (SEM). XRD patterns of TiO_2 nanorods and nanoparticles were carried out on a Siemens D5000 X-ray diffractometer (XRD) using CuKα radiation.

Characterization of PVC/TiO_2 Nanocomposites

Tensile test measurements. Tensile tests were performed at room temperature (25°C) according to ASTM D638 using the tensile testing machine (Zwick-Roell Z010). The samples before and after irradiation were tested at a crosshead speed of 10 mm/min. The reported values are the average of six measurements on specimens, were taken from the same direction of molded samples.

FTIR spectroscopy. Fourier transform infrared (FTIR) analysis were performed at room temperature (25°C) using the FTIR spectrometer (UNICAM Matson 100, England). Samples were tested before and after UV irradiation in order to assess the extent of degradation in the nanocomposites. The IR spectra

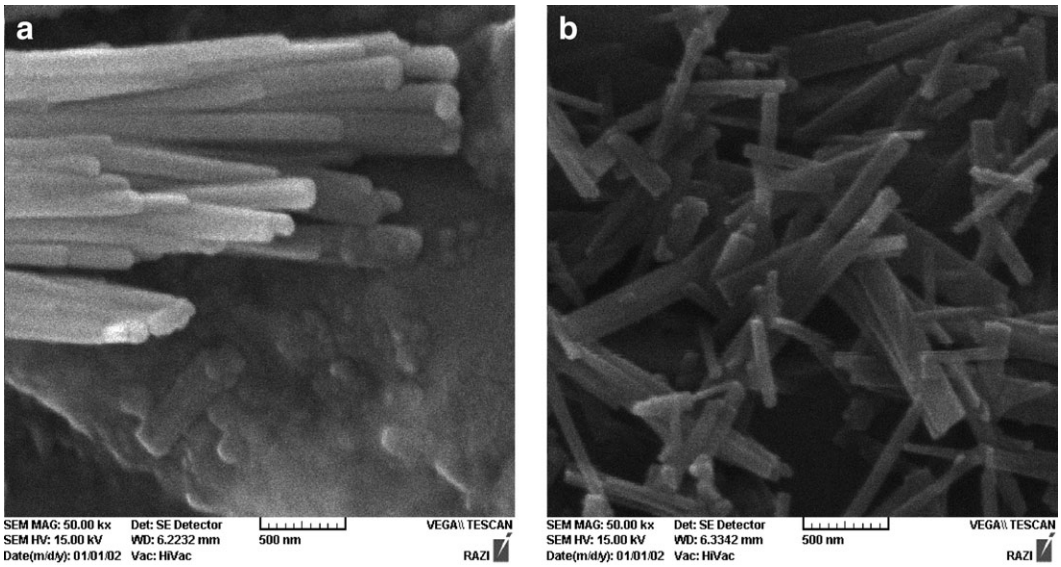

Figure 1. SEM micrographs of nanorods samples: (a) PTi1 and (b) PTi2.

were recorded in absorbance mood from the 1500–1900 cm^{-1} range; the peak area of the carbonyl and polyene bands were used to estimate photodegradation by using the Essential FTIR software (Operant LLc, Version 1.1.0.0).

Contact angle measurement. Contact angles of two liquids (normal decane and deionized water) on PVC film before and after irradiation were measured at room temperature (25°C), with contact angle measurement apparatus made in our laboratory, equipped with optical microscope (TZM-2 model, BEL, Italy). The liquid droplet (2 μL) was placed onto the polymer surface by a micro syringe. The droplet image was recorded, and then contact angle of each drop was measured by Image-J software. Each contact angle is the average of minimum five measurements. The surface tension (γ_s) and their dispersive (γ_s^D) and polar (γ_s^P) components were calculated using the Fowkes methods.[21]

RESULTS AND DISCUSSION

Nanorods Properties

Figure 1 shows the scanning electron microscopy (SEM) micrographs of the nanorod samples. Average l/d values of nanorods determined by Image-J software and specific surface area of the TiO_2 nanorods and nanoparticles are reported in Table I. Obviously, PTi1 nanorods have higher aspect ratio and lower specific surface area compared to those of PTi2 nanorods which can be effective factors on mechanical properties of the nanocomposites.

Figure 2 shows XRD patterns of TiO_2 nanorods and nanoparticles confirming the formation of amorphous (noncrystalline) structures in the synthesized TiO_2 nanorods. While in XRD pattern of TiO_2 nanoparticles, the picks of anatase and rutile crystalline structures is observed clearly. This trend reveals that photocatalytic properties of TiO_2 nanorods can be lower than that of TiO_2 nanoparticles.

Mechanical Properties of Nanocomposites

Yield stress of PVC nanocomposites with the presence of TiO_2 nanorods and nanoparticles before and after UV exposure compared with unfilled PVC, are shown in Figure 3. It should be noted that the yield stress for unfilled PVC is much less than that of the nanocomposites.

The expression for the yield stress of (nano)composites was first reported as follows by Nardone et al.:[22]

$$\sigma_{c,y} = \sigma_{m,y}\left[\frac{1}{2}\phi_P\left(2+\frac{l}{d}\right)+1-\phi_P\right] = \sigma_{m,y}\left[1+\frac{l}{2d}\phi_P\right] \quad (1)$$

where $\sigma_{c,y}$ and $\sigma_{m,y}$ are the yield stress of (nano)composite and matrix, respectively; l/d and ϕ_P are the aspect ratio and volume fraction of nanorods, respectively; d is the diameter and l is the length of the nanorods. The above formula shows that the yield stress of the nanocomposite increase with increasing of the nanorods aspect ratio.[22]

An alternative relationship commonly used for micron-sized rigid particles is given as eq. (2):[10]

$$\sigma_{c,y} = \sigma_{m,y}\left(1-1.21\phi_P^{\frac{2}{3}}\right) \quad (2)$$

The yield stress of the NP1 and NP2 nanocomposites was also calculated using eq. (1) and the yield stress of the NP3 nanocomposites was calculated from eq. (2) as presented in Figure 3. The results of eq. (1) are in good agreement with experimental data, but the correlation of eq. (2) with experimental data is poor.

Moreover, the mechanical properties before and after UV exposure, confirmed that the presence of TiO_2 nanorods improves the yield stress of PVC nanocomposites compared with unfilled PVC. This behavior is attributed to the nanorods special geometric shapes and their high aspect ratio (l/d) which being able to result in unique properties in PVC matrix.

Applied Polymer SCIENCE

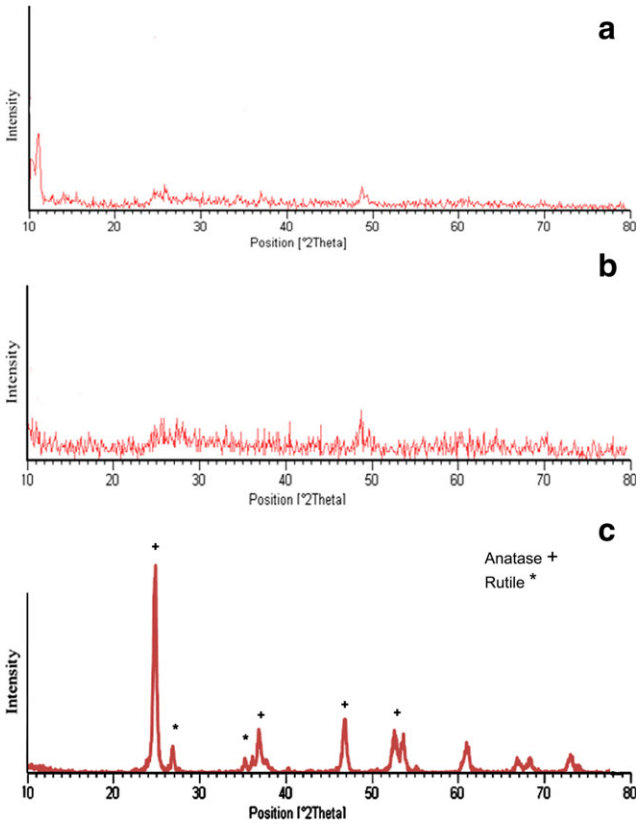

Figure 2. XRD patterns of TiO_2: (a) PTi1 (b) PTi2 (c) P25. [Color figure can be viewed in the online issue, which is available at wileyonlinelibrary.com.]

The comparison of the results before and after exposure show that nanorods lead to an improvement in the photostability of PVC nanocomposites. This trend can be related to the amorphous structure of the synthesized nanorods. High photocatalytic activity and high surface area of the TiO_2 nanoparticles (Degussa P25), cause more degradation in PVC matrix and more reduction in yield stress after UV exposure.

Modulus of elasticity of the nanocomposites at the presence of TiO_2 nanorods and nanoparticles before and after UV exposure compared to unfilled PVC are presented in Figure 4. It should be mentioned that the modulus of unfilled PVC is much less than that of the nanocomposites.

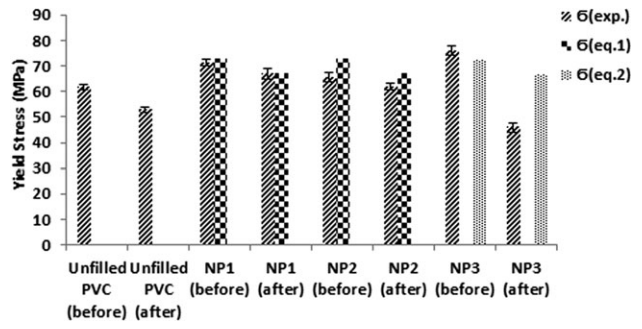

Figure 3. Yield stress of nanocomposites before and after UV exposure.

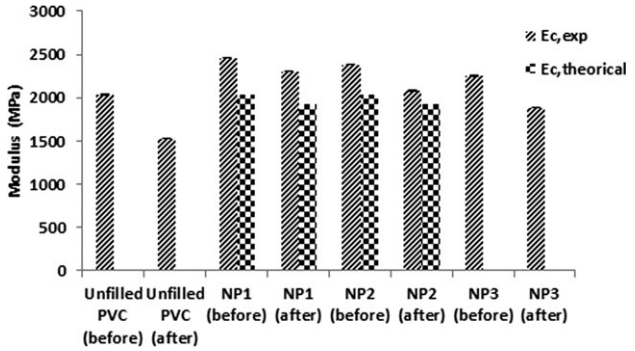

Figure 4. Elastic modulus of nanocomposites before and after UV exposure.

Increases in modulus of rigid particulate filled polymer composites can be predicted well by Nielsen's modified Kerner's equation, as described by eq. (3):[23]

$$E_c = E_m\left(\frac{1+AB\phi_p}{1-B\psi\phi_p}\right) \tag{3}$$

$$\psi = 1+\left[\frac{1-\phi_m}{\phi_m^2}\right]\phi_P \tag{4}$$

$$A = K_E - 1 \tag{5}$$

where E_c and E_m are the composites' and matrix's elastic moduli, respectively. ϕ_P is the volume fraction of filler. A is a constant dependent on the geometry of the nanorod and the Poisson's ratio of the matrix, which was calculated to be 6.2 and 4.9 for PTi1 and PTi2, respectively assuming a Poisson's ratio of 0.4.[24] B is a constant dependent on the relative stiffness of the particulate filler and the matrix, which was calculated to be close to 1 due to high filler to matrix modulus ratio. ψ is a reduced concentration term which depends upon the maximum packing fraction $\phi_m$of the nanorod in the polymer (values of $\phi_m$are tabulated in Ref. 23). The theoretical results are in good agreement with experimental data (see Figure 4).

It should be mentioned that with increasing the aspect ratio (l/d) of TiO_2 nanorods, the load transfer capacity from polymeric matrix to filler is increased and this issue leads to the improvement of elastic modulus and yields stress of the nanocomposites. The mechanism of stress distribution of nanorod–polymer nanocomposites was found to be analogous to that in fiber-reinforced composites. It is commonly accepted that the addition of spherical TiO_2 nanoparticles can lead to increase in the yield stress and elongating at break of the NP3 nanocomposite, but TiO_2 nanoparticles cannot intensify the elasticity modulus of NP3 compared with NP1 and NP2 nanocomposites because of their low aspect ratio.

The reduction in modulus of nanocomposites after UV exposure can be attributed to the chain scission in PVC matrix which is as a result of photodegradation process, but this trend increases in NP3 nanocomposite. The reason of this behavior is related to the mixed-phase titania in TiO_2 nanoparticles (Degussa P25) that shows greater photocatalytic activity due to three factors:[25]

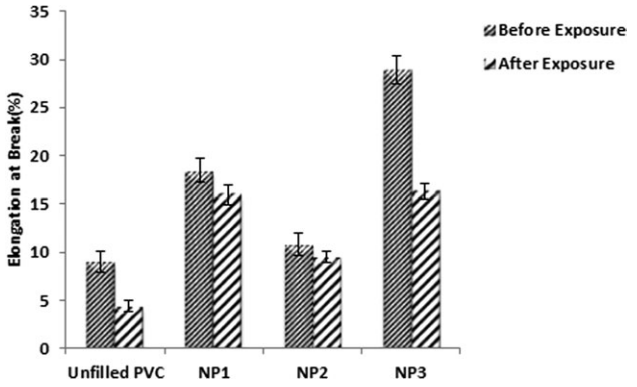

Figure 5. Elongation at break of nanocomposites before and after UV exposure.

(a) the smaller band gap of rutile, extending the useful range of photoactivity into the visible region; (b) the stabilization of charge separation by electron transfer from rutile to anatase slows recombination; and (c) the small size of the rutile crystallites facilitates this transfer, making catalytic "hotspots" at the rutile/anatase interface.

Mechanical properties, especially tensile strength of the composites are significantly affected by the interfacial adhesion between the particulate fillers and matrix. Pukanszky et al.[26] developed a model to predict the variation in the composite's tensile strength with the particulate filler content:

$$\sigma_{c,y} = \sigma_{m,y}(1 - \phi_P) \exp \frac{\beta \phi_P}{1 + 2.5\phi_P} \tag{6}$$

where $\sigma_{c,y}$ and $\sigma_{m,y}$ represent the tensile strength of the nanocomposites and unfilled polymer, respectively, ϕ_P represents the volume fraction of filler, and β is a semi-empirical parameter that accounts for the macroscopic characteristics of the interface, affecting the tensile strength of nanocomposite. The value of the β parameter reflects the interfacial adhesion between the particles and polymeric matrix. A higher value of β corresponds to a stronger interfacial adhesion between them.[27]

The calculated values of β are 3.79 for NP1, 1.69 for NP2 and 7.89 for NP3 nanocomposites. These differences in the β values can be related to the high specific surface area of the fillers. This trend is in good agreement with the tensile properties of nanocomposites.

The result of elongation at break for the nanocomposites at the presence of TiO_2 nanorods and nanoparticles before and after UV exposure compared to unfilled PVC are presented in Figure 5. The elongation at break for unfilled PVC is much less than that of the nanocomposites. The addition of nanorods and nanoparticles to PVC increases the elongation at break. Furthermore, the low elongation at break of NP1and NP2 samples in comparison with NP3 nanocomposite can be related to the high modulus and rigidity of the nanocomposites consist of TiO_2 nanords. The results of the elongation at break for nanocomposites reveals a considerable decrease in elongation at break in NP3 sample after UV exposure, but nanocomposites containing nanorods show the highest resistance after UV exposure. Irradiation causes chain scission in PVC structure and reduces elongation at break of nanocomposites. This behavior can be assimilated to a ductile to brittle transition spread over time.[28] But the presence of nanorods in PVC matrix results in a significant decrease of this reduction. This fact is very important in manufacturing of photo stable outdoor PVC articles.

FTIR Analyses of Nanocomposites

The functional groups in the nanocomposite films were monitored by FT-IR analysis. Figure 6 shows the changes in the FTIR spectra of the nanocomposite films before and after UV exposure. The main differences which were observed in these absorption spectra are related to the polyene (1600–1680 cm^{-1}) and carbonyl (1680–1780 cm^{-1}) groups. For all of the nanocomposites films, intensities of the polyene and carbonyl groups absorption peaks increase after UV irradiation time. Furthermore, polyene index was calculated by subtracting the value of the integrated surface area of the absorption bands at 1630 cm^{-1} from the baseline and dividing it by the reference value of the integrated surface area of the absorption bands at 2920 cm^{-1} subtracted from the baseline as shown in eq. (7).[29,30] The different wave numbers followed were 2920 and 1650 cm^{-1} for C-H stretching and polyene sequences, respectively. For carbonyl index, it was calculated according to eq. (8). The wave number of 1730 cm^{-1} represents carbonyl groups; Where A_{1730} is the integrated surface area of the absorption bands at 1730 cm^{-1}. The results of calculated polyene and carbonyl indexes are presented in Figures 7 and 8.

$$\text{Polyene index} = \frac{(\%A_{1650} - \%A_{\text{baseline}})}{(\%A_{2920} - \%A_{\text{baseline}})} \tag{7}$$

$$\text{Carbonyl index} = \frac{(\%A_{1730} - \%A_{\text{baseline}})}{(\%A_{2920} - \%A_{\text{baseline}})} \tag{8}$$

As can be seen in the Figures 7 and 8, the polyene and carbonyl indexes for nanocomposites increase after UV irradiation. The increase in polyene sequences can probably due to a photodegradation of PVC nanocomposites. Furthermore, the increasing intensities of the carbonyl groups suggest that the photooxidation reaction has taken place in the composite film. In the composite film, TiO_2 nanoparticles can be excited by UV light to generate active electron-hole pairs, which can react with the surface-absorbed molecules and form active oxygen species. Then, these active oxygen species oxidize C—H groups to form C=O groups.[31] However, the increasing intensities of the polyene and carbonyl groups in the NP3 nanocomposite film are more pronounced than those of the NP1 and NP2 nanocomposite films. The reason of this behavior is related to the mixed-phase titania in TiO_2 nanoparticles (Degussa P25) in the NP3 nanocomposite that shows greater photocatalytic activity due to three factors that can be related to the structure of TiO_2 nanoparticles as mentioned in Mechanical Properties of Nanocomposites.[25]

Contact Angle of Nanocomposites

The method of static contact angle (θ) (Sessile drop) measurement was used to calculate the polymer surface tension. Photographic image for contact angel measurements of the nanocomposites before and after UV exposure are represented in Figure 9.

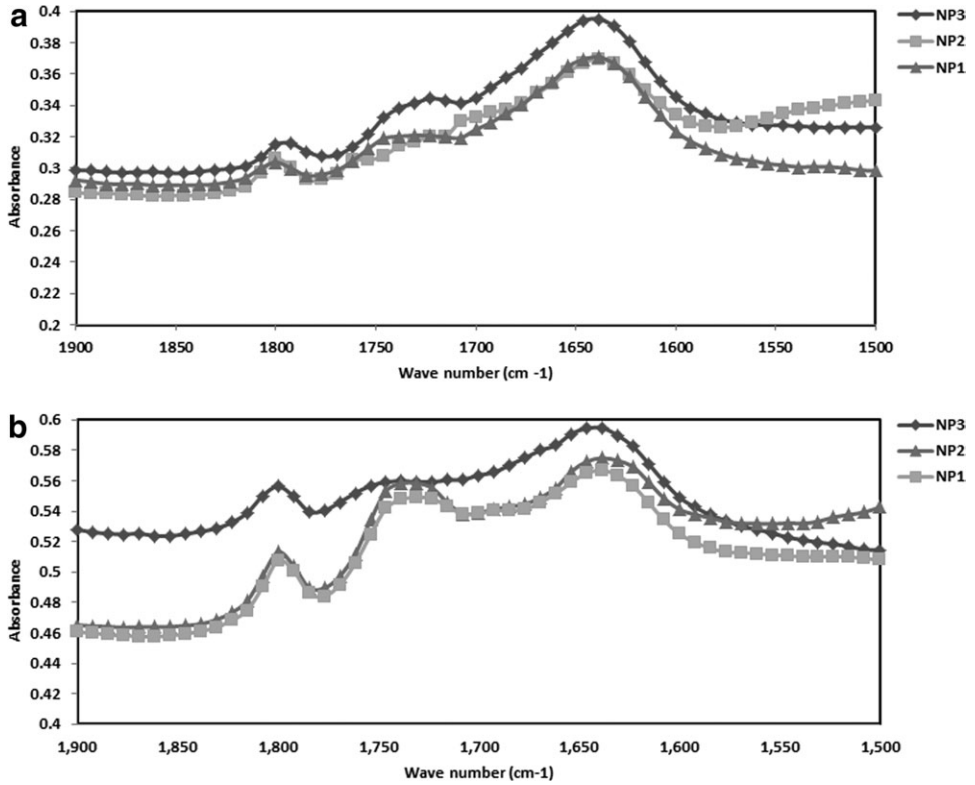

Figure 6. FTIR spectrum of nanocomposites (a) before and (b) after UV exposure.

The changes in the contact angle and surface tension in UV-irradiated nanocomposites are presented in Tables II and III. Contact angle is a measure of noncovalent forces between liquid and the first monolayer of material. Thus, in the case of strong interaction between phases, the liquid drop spreads on the solid and wets it. The quality of the surface, its roughness and porosity strongly influences contact angle values. The wettability of n-decane on PVC is much higher (small θ values) than water (higher θ values), because the molecules of a highly polar liquid are less attracted by PVC macromolecules, which has a relatively low polarity.[32]

The results of the contact-angle measurements were analyzed according to the following theory in order to estimate of the dispersive and polar components of the surface tension of the samples. The Young equation gives the following relationship for the contact angle (Θ):

$$\gamma_S = \gamma_{SL} + \gamma_L \cos\theta \tag{9}$$

where γ_S is the surface tension of the solid, γ_L is that of liquid, and γ_{SL} is the interfacial tension between the solid and liquid. The surface tension of a liquid is numerically the same as its surface energy per unit area. The surface energies of both solid and liquid are the sum of dispersive component (distinguished by superscript D) and polar component (distinguished by superscript P), as follows:

$$\gamma_S = \gamma_S^D + \gamma_S^P \tag{10}$$

$$\gamma_L = \gamma_L^D + \gamma_L^P \tag{11}$$

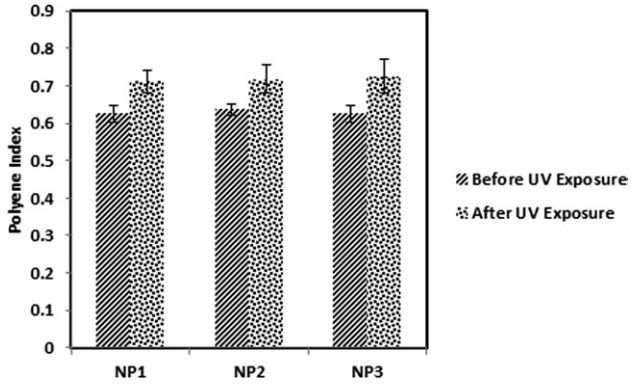

Figure 7. Polyene index of nanocomposites before and after UV exposure.

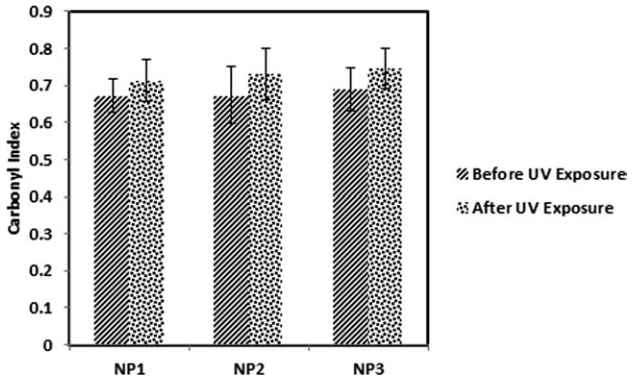

Figure 8. Carbonyl index of nanocomposites before and after UV exposure.

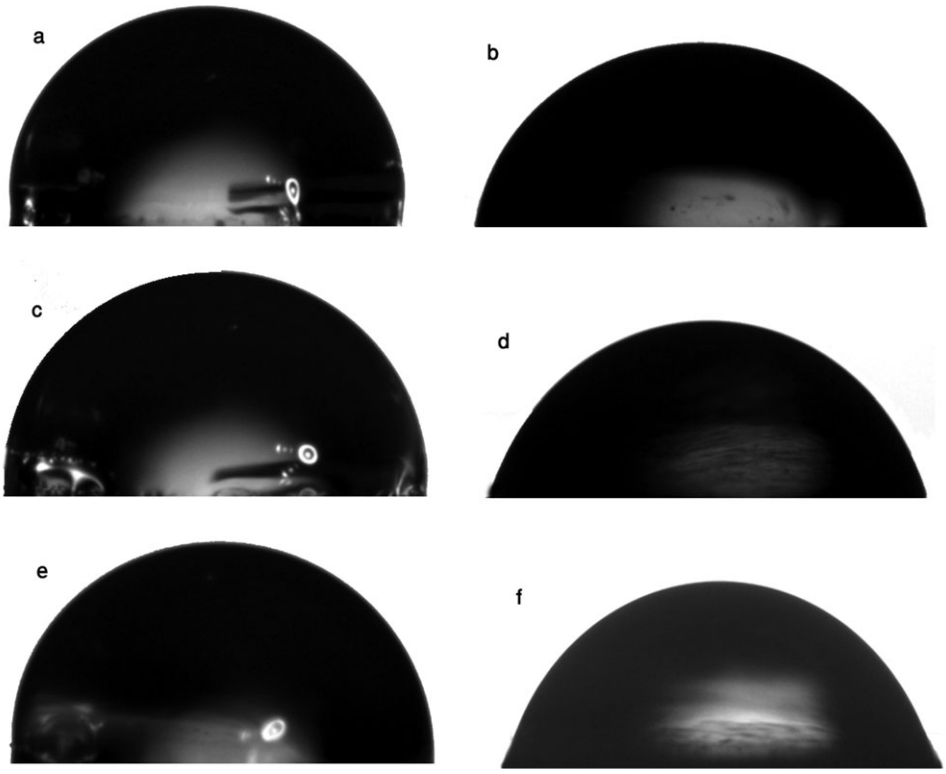

Figure 9. Contact angel measurements of the nanocomposites before and after UV exposure (a) NP1 (before), (b) NP1 (after), (c) NP2 (before), (d) NP2 (after), (e) NP3 (before) and (f) NP3 (after).

Fowkes gives the following equation for the interfacial tension in terms of the surface tensions of the two surfaces which form the interface:[21]

$$\gamma_{SL} = \gamma_S + \gamma_L - 2\left(\gamma_S^D \gamma_L^D\right)^{1/2} - 2\left(\gamma_S^P \gamma_L^P\right)^{1/2} \quad (12)$$

Equation 9 and 12 can be combined to give:

$$\frac{\gamma_L(1+\cos\theta)}{2\left(\gamma_L^D\right)^{1/2}} = \left(\gamma_S^P\right)^{1/2} \frac{\left(\gamma_L^P\right)^{1/2}}{\left(\gamma_L^D\right)^{1/2}} + \left(\gamma_S^D\right)^{1/2} \quad (13)$$

This means that if $\frac{\gamma_L(1+\cos\theta)}{2\left(\gamma_L^D\right)^{1/2}}$ is plotted against $\frac{\left(\gamma_L^P\right)^{1/2}}{\left(\gamma_L^D\right)^{1/2}}$, the graph would be linear with intercept $\left(\gamma_S^D\right)^{1/2}$and slope $\left(\gamma_S^P\right)^{1/2}$. Values of the dispersive and polar components of surface tensions were collected in Table III.

In accordance to Table II, the contact angle values show a decrease for water and an increase for n-decane, as a solvent, after UV exposure. A decrease in contact angle values demonstrated on better dispersion of solvent on the surface and the better dispersion means better consistency with surface. As it is known, water is a polar and n-decane is a nonpolar fluid, therefore the trend from contact angle measurements confirms increasing of surface hydrophilicity after UV exposure. But as can be observed in Table III, after UV exposure to the samples, the dispersive component of surface tension shows a little decrease although the polar component increases significantly. So variation in surface tensions values comes from the changes in their polar component. This increase in surface tensions

Table II. Contact Angle Values for Samples with Different Solvents Before and After UV Exposure

		Contact angle (°)	
Sample	Exposure mode	Water	n-Decane
NP1	Before	87.5	20.1
	After	70.6	22.2
NP2	Before	87	21.9
	After	68.9	23.6
NP3	Before	85.1	17.5
	After	65.7	20.8

Table III. Surface Tension of Samples Obtained from Contact Angle Values

Sample	Exposure mode	γ_S^P (mJ/ m^2)	γ_S^D (mJ/ m^2)	γ_S (mJ/ m^2)
NP1	Before	4.9	22.4	27.3
	After	13.8	22.1	35.9
NP2	Before	5.2	22.1	27.4
	After	15.1	21.9	36.9
NP3	Before	5.8	22.7	28.6
	After	16.9	22.3	39.2

demonstrated an increase on polarity of surface; which is attributed to the formation of polar groups and enrichment of surface with functional groups.[33] This significant increase of PVC polarity indicates that an efficient oxidation on polymer surface occurs. The polymer surface is activated by UV irradiation, which explains such efficient oxidation. This leads to the formation of different types of carbonyl, hydroxyl, and hydroperoxide groups that strongly influences γ_S^P and γ_S^D, therefore encounter more hydrophilicity to the samples after UV exposure. Another reason is the possibility of formation of small cracks, crazes and voids, after UV exposure which influences the contact angle measurements. In NP1 and NP2 nanocomposites decrease in contact angle and surface tension are less than that in NP3 nanocomposite. These results reveal good photostability potential of these nanocomposites in comparison with NP3 nanocomposite, which can be related to the amorphous structure of nanorods and high photocatalytic property of nanoparticles.

CONCLUSIONS

PVC nanocomposites filled with different types of TiO_2 nanostructures (nanorods and nanoparticles) were prepared via a melt blending method. The results of tensile measurements showed that the presence of TiO_2 nanorods led to an improvement in mechanical properties of PVC nanocomposite in comparison with unfilled PVC before and after UV exposure. The contact angle and surface tension measurement results indicated that, increase in the polar component (γ_S^P) of PVC is attributed to the formation of polar groups in the photo degraded PVC after exposure, but this increasing in the polar component is not significant in PVC nanocomposites with the presence of TiO_2 nanorods compared to those with TiO_2 nanoparticles. Furthermore, the results of the FTIR analyses confirmed this consequence. The obtained results illustrated that the samples consist of titanium dioxide nanorods have lower photocatalytic property which can be due to their amorphous structure, confirming highly effect of the synthesized nanorods on the photostabilization of PVC matrix.

REFERENCES

1. Kaczmarek, H.; Kowalonek, J.; Oldak, D. *Polym. Degrad. Stabil.*, **2003**, *79*, 231.
2. Kaczmarek, H.; Swiatek, M.; Kaminska, A. *Polym. Degrad. Stabil.* **2004**, *83*, 35.
3. Pimentel Real, L. E.; Ferraria, A. M.; Botelho do Rego, A. M. *Polym. Test.* **2008**, *27*, 743.
4. Liu, Z. H.; Zhang, X. D.; Zhu, X. G.; Li, R. K. Y.; Wang, F. S.; Choy, C. L. *Polymer* **1998**, *39*, 5047.
5. Wong-On, J.; Wootthikanokkhan, J. *J. Appl. Polym. Sci.* **2003**, *88*, 2657.
6. Whittle, A. J.; Burford, R. P.; Hoffman, M. J. *Plastics Rubber Compos.* **2001**, *30*, 434.
7. Crawford, E.; Lesser, A. J. *Polymer* **2000**, *41*, 5865.
8. Nakamura, Y.; Fukuoka, Y.; Iida, T. *J. Appl. Polym. Sci.* **1998**, *70*, 311.
9. Gilbert, M.; Hitt, D. J.; Schmaucks, G.; Fried, B.; Sorhuus, A.; Roszinski, J. O. *Plastics Rubbers Compos.* **2005**, *34*, 94.
10. Kemal, I.; Whittle, A.; Burford, R.; Vodenitchorova, T.; Hoffman, M. *Polymer* **2009**, *50*, 4066.
11. Dong, Z.; Manimala, J. M.; Sun, C. T. *J. Mech. Mater. Struct.* **2010**, *5*, 529.
12. Chen, X.; Mao, S. S. *Chem. Rev.* **2007**, *107*, 2891.
13. Watson, S.; Beydoun, D.; Scott, J.; Amal, R. *J. Nanoparticle Res.* **2004**, *6*, 193.
14. Yang, J.; Mei, S.; Ferreira, J. M. *Mater. Sci. Eng.* **2001**, *15*, 183.
15. Neupane, M. P.; Park, S.; Lee, M. H.; Bae, T. S.; Watari, F. *Bio-Med. Mater. Eng.* **2009**, *19*, 77.
16. Li, G.; Liu, Z.; Zhang, Z.; Yan, X. *Chinese J Catalysis.* **2009**, *30*, 37.
17. Bavykin, D. V.; Parmon, V. N.; Lapkin, A. A.; Walsh, F. C. *J. Mater. Chem.* **2004**, *14*, 3370.
18. Anton-Prinet, C.; Mur, G.; Gay, M.; Audouin, L.; Verdu, J. *Polym. Degrad. Stab.* **1998**, *61*, 211.
19. Gesenhues, U. *Polym. Degrad. Stabil.* **2000**, *68*, 185.
20. Dufresne, A.; Paillet, M.; Putaux, J. L.; Canet, R.; Carmona, F.; Delhaes, P.; Cui, S. *J. Mater. Sci.* **2002**, *37*, 3915.
21. Comyn, J.; Blackley, D. C.; Harding, L. M. *Int. J. Adhesion Adhesives.* **1992**, *13*, 163.
22. Nardone, C. V.; Prewo, M. *Scripta Materialia.* **1986**, *20*, 43.
23. Nielsen, L. E. Mechanical Properties of Polymers and Composites; Marcel Dekker: New York, **1974**; Vol. *2*, Chapter 7, p 379.
24. Erhad, G. Designing with Plastics; Hanser: Munich, Germany, **2006**; Chapter 4, p 125.
25. Kemp, T. J.; McIntyre, R. A. *Polym. Degrad. Stabil.* **2006**, *91*, 165.
26. Vörös, G.; Fekete, E.; Pukanzsky, B. *J. Adhesion* **1997**, *64*, 229.
27. Sun, S.; Li, C.; Zhang, L.; Du, H. L.; Burnell-Gray, J. S. *Polym. Int.* **2006**, *55*, 158.
28. Anton-Prinet, C.; Mur, G.; Gay, M.; Audouin, L.; Verdu, J. *J. Mater. Sci.* **1999**, *34*, 379.
29. Chaochanchaikul, K.; Sombatsompop, N. *Polym. Eng. Sci.* **2011**, *51*, 1354.
30. Shi, W.; Zhang, J.; Shi, X. M.; Jiang, G. D. *J. Appl. Polym. Sci.* **2008**, *107*, 528.
31. Yang, C.; Deng, K.; Peng, T.; Zan, L. *Chem. Eng. Technol.* **2011**, *34*, 886.
32. Kaczmarek, H.; Kowalonek, J.; Szalla, A. *Surface Sci.* **2002**, *507*, 833.
33. Chen, X.; Wang, Y.; Shen, J. *Polym. Degrad. Stabil.* **2005**, *87*, 527.